

Regioselective Ring-Opening of Oxetanes Catalyzed by Lewis Superacid $\text{Al}(\text{C}_6\text{F}_5)_3$

Marina Bellido,^{a, b} Carlos Riego-Mejías,^{a, b} Giuseppe Sciortino,^c
Xavier Verdager,^{a, b,*} Agustí Lledós,^{c,*} and Antoni Riera^{a, b,*}

^a Institute for Research in Biomedicine (IRB Barcelona), The Barcelona Institute of Science and Technology (BIST), Baldiri Reixac, 10. 08028 Barcelona, Spain

E-mail: antoni.riera@irbbarcelona.org

^b Departament de Química Inorgànica i Orgànica, Secció Química Orgànica, Universitat de Barcelona, Martí i Franquès 1, 08028 Barcelona, Spain

^c Departament de Química, Universitat Autònoma de Barcelona, Cerdanyola del Vallès, 08193 Barcelona, Spain
E-mail: agusti.lledos@uab.cat

Manuscript received: October 16, 2023; Revised manuscript received: January 2, 2024;

Version of record online: ■■, ■■

Dedicated to our colleague and friend Miquel A. Pericàs for his scientific contributions, on the occasion of his retirement from the ICIQ



Supporting information for this article is available on the WWW under <https://doi.org/10.1002/adsc.202301183>

© 2024 The Authors. Advanced Synthesis & Catalysis published by Wiley-VCH GmbH. This is an open access article under the terms of the Creative Commons Attribution Non-Commercial NoDerivs License, which permits use and distribution in any medium, provided the original work is properly cited, the use is non-commercial and no modifications or adaptations are made.

Abstract: This study details an aluminum-catalyzed regioselective isomerization of 2,2-disubstituted oxetanes to yield homoallylic alcohols. The reaction takes place in toluene at 40 °C, employing 1 mol% of $\text{Al}(\text{C}_6\text{F}_5)_3$ as catalyst. This catalytic system shows a wide substrate scope (12 examples). The optimized conditions are especially useful for electron-rich aryl oxetanes, completely suppressing the formation of allyl isomers and reducing the amount of the dimer by-product. The synthetic applicability of the reported methodology is demonstrated by the enantioselective formal synthesis of curcuminone and the $\sigma 1$ receptor agonist RC-33.

Keywords: Lewis superacid; tris(pentafluorophenyl)alane; oxetanes, isomerization; catalysis, asymmetric hydrogenation; natural product synthesis

Introduction

Precious metals have demonstrated outstanding efficacy in homogeneous catalysis, contributing significantly to numerous total syntheses.^[1,2] However, there is an increasing need for catalytic transformations that are not reliant on costly transition metals.^[3] Consequently, interest in the exploration of catalysts derived from first-row and main-group abundant metals is growing. Lewis acid (LA) catalysis illustrates the expanding landscape of this field.^[4]

LAs are molecules that can accept an electron pair in their vacant orbital.^[5] The term “Lewis superacid”, introduced by Olah, categorizes those acids stronger

than anhydrous AlCl_3 .^[6] Krossing and coworkers later proposed as a definition those LA that are stronger than monomeric SbF_5 in gas phase.^[7] There are several ways to measure the strength of an LA. In general, they involve a compromise of attractive (electrostatic, covalent, dispersive) and repulsive interactions. Greb recently reported an extensive study classifying the Lewis superacidity of a collection of strong LAs.^[8] In this regard, compounds ER_3 with elements of group 13 (B, Al, Ga, In, Tl) have been used multiple times as canonical LAs.^[9]

One of the most common strategies to fine tune the properties of acids in order to convert them into Lewis superacids is by employing electron-withdrawing sub-

stituents ($R=EWG$). Numerous successful examples can be found in the chemistry of LAs bearing fluorinated aryl substituents, denoted as $E(Ar^F)$.^[10,11]

While $B(C_6F_5)_3$ is well known and widely employed, the chemistry of $Al(C_6F_5)_3$ has been less explored. A comprehensive comparison between $B(Ar^F)_3$ and $Al(Ar^F)_3$ was recently published by Kaehler and Melen.^[12] They based the study on the syntheses, properties and reactivity of these compounds. $Al(C_6F_5)_3$ was first prepared by metathesis of mixed aluminum organyls (Me_2AlCl and LiC_6F_5).^[13] The development of novel reactivity for the alane analogue was initially hampered by its stability; an explosion was described during attempts to purify the compound by sublimation.^[14] Consequently, nowadays it is prepared as a toluene adduct by transmetalation from its borane counterpart.^[15] Despite its potential sensitivity, $Al(C_6F_5)_3$ is widely used as catalyst in polymerization reactions.^[16]

Although there is some controversy in the literature, the consensus suggests that triarylalanes are stronger LAs than the analogous boranes.^[17] A theoretical study developed by Timoshkin *et al.*,^[10] supports this hypothesis through the observation of the highest reorganization energy in boron as compared to aluminum.^[18] This energy is the one required for the geometrical modification ($E-C$ bond elongation) upon coordination: transitioning from trigonal planar geometry to a pyramidal conformation. Due to the smaller size and shorter $B-C$ bonds of boron, its complexes exhibit higher repulsion between the organic residues compared to Al -based LAs. Berionni and coworkers experimentally measured this high reorganization energy for $B(Ar^F)_3$.^[19] A proof of the stronger acidity of $Al(C_6F_5)_3$ is that it can form adducts even with weak bases like toluene, while the borane analogue lacks this capacity.^[20]

Over the past years, our group has focused on the Ir -catalyzed regioselective isomerization of strained heterocycles: N -sulfonyl aziridines to terminal allylic amines,^[21] and epoxides to aldehydes, known as the Meinwald rearrangement.^[22] These reactions show perfect atom economy, and in the case of allyl amines, they yielded excellent substrates for asymmetric hydrogenation (AH).

While molecules containing oxetanes have recently gained relevance in medicinal chemistry applications,^[23] there is still room for further exploration of their derivatization.^[24] Notably, the ring-opening of oxetanes has been extensively studied for reactions involving ring expansion to carbonates, catalyzed by Fe or Al .^[25] Furthermore, successful reductive ring-opening has been achieved using Ti as catalyst.^[26] Recent advancements include the application of Co-catalysis for the ring expansion/ring opening of oxetanes.^[27]

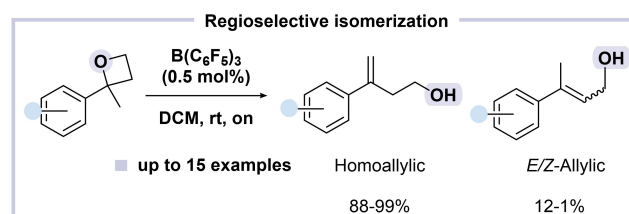
Oxetanes are less reactive than their three-membered ring analogues,^[28] and this property hampers their ring-opening with Ir -based Crabtree's catalyst. To expand the reactivity of this strained heterocycle, our group reported the regioselective ring-opening of 2,2-disubstituted oxetanes to homoallylic alcohols using the bulky Lewis superacid $B(C_6F_5)_3$ (Scheme 1).^[29] We found that this commercially available LA, could be employed to control the regioselectivity between the homoallylic and the (E/Z)-allylic products that were formed (Scheme 1). The regioselectivities to the homoallylic alcohol ranged from 88% to 99%. However, the amount of oligomeric by-products was not determined.

Despite the excellent regioselectivities of this reaction, we observed two main drawbacks namely the difficult separation of allylic alcohols from the desired homoallylic products and the substantial formation of a dimer by-product. The first issue lowered the enantiomeric excess in the next AH step. As a result, only 5 of the 15 examples were hydrogenated in the previous work. The other weakness lowered the yield and was a significant problem when using electron-rich oxetanes.

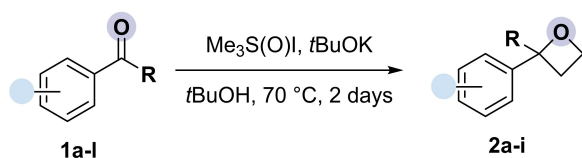
Although, in some cases, the first limitation could be addressed by the derivatization to the corresponding homoallylic sulfones, which provides crystallinity and eases the separation of the isomers,^[30] we attempted to solve both drawbacks by improving the reactions conditions. We report herein an improved procedure for the regioselective oxetane ring-opening using the Lewis superacid $Al(C_6F_5)_3$. This approach suppressed the formation of the regioisomeric allyl alcohols and reduced the dimer formation, expanding the scope to electron-rich homoallylic alcohols. The applicability of this methodology is shown by the formal synthesis of curcumin and the total synthesis of RC-33.

Results and Discussion

All 2,2-disubstituted oxetanes **2** used in this article, including those bearing electron-donating substituents in the phenyl ring, were synthesized from acetophenones **1a–l** by a double Corey-Chaykovsky reaction (Scheme 2).^[31]



Scheme 1. Regioselective isomerization of oxetanes using $B(C_6F_5)_3$ as the catalyst.



Scheme 2. Transformation from ketones to oxetanes.

Our initial explorations started from the optimization of the reaction conditions using *p*-methoxyphenyl oxetane **2a** as our model substrate (Table 1).

Given that we had already tested several LAs,^[29] here we focused on Al-based LAs (Table 1). The previous conditions, using $B(C_6F_5)_3$ afforded a 67:12:21 ratio of products (entry 1, Table 1). We should note that 21% molar ratio of dimer means 35% in weight. Somewhat surprisingly, $AlCl_3$ showed poorer regioselectivity but less dimerization product **5a** (entry 2, Table 1). Consequently, we proposed a bulkier aluminum LA with electron-rich ligands (entries 3 and 4, Table 1). Although dimerization was quite low, the regioselectivity and the conversion were still poor, with substantial amounts of allylic alcohols **4a**. Finally, using $Al(C_6F_5)_3$ (entry 5, Table 1), a bulky LA with electron-withdrawing substituents, the conversion was complete and the formation of the allylic isomers **4a** and dimer **5a** was reduced with respect to the boron analogue.

Superacid $Al(C_6F_5)_3$ was easily prepared by transmetallation from $B(C_6F_5)_3$.^[32,33] To increase the stability of this superacid, it was prepared in a 1:3 solution of anhydrous toluene/hexane by adding 1 equiv. of $AlMe_3$ to a suspension of $B(C_6F_5)_3$. In this way, the toluene adduct,^[33,34] $Al(C_6F_5)_3 \cdot tol$, was filtered and used under strict anhydrous and inert conditions.^[35]

Table 1. Screening of catalysts in the regioselective oxetane ring-opening reaction.

Entry	Lewis Acid	Conv	3a ^[a]	4a ^[a]	5a ^[a]
1	$B(C_6F_5)_3$	100	67	12	21
2	$AlCl_3$	100	50	39	11
3	$AlEt_2CN$	15	82	12	7
4	$AlEt_3$	15	67	23	10
5	$Al(C_6F_5)_3$	100	88	4	8

^[a] Molar ratio determined by ¹H-NMR.

Once we had selected the LA, we proceeded to further optimize the ring-opening reaction. We expected that the solvent effect would be pivotal in the outcome of the isomerization reaction due to the huge coordinating strength of $Al(C_6F_5)_3$.^[20] We realized that $Al(C_6F_5)_3 \cdot tol$ had to be freshly prepared before its use as it degraded over time, even when stored at low temperatures under N_2 . In addition, we observed that the colour of the $Al(C_6F_5)_3 \cdot tol$ solution changed depending on the solvent. For example, orange or red solutions were obtained with DCM and $CDCl_3$, respectively, whereas the treatment of $Al(C_6F_5)_3$ with C_6D_6 gave a colourless solution. Chakraborty and Chen suggested that the yellow solution in DCM, corresponds to the formation of an $Al(C_6F_5)_2Cl$, which could be the actual catalytic species in this solvent.^[36] We also found that the purity of the oxetanes was crucial for the success of the reaction since small amounts of impurities can decompose the catalyst. Therefore, all oxetanes were purified by column chromatography to afford transparent oils.

Table 2 summarizes the different parameters that were assessed starting from DCM as the initial point (entry 1). Other chlorinated solvents, such as DCE or $CHCl_3$, also gave good results (entry 3 and 4, respectively). Ether solvents, such as THF or TBME^[37] (entry 5 and 6), yielded good selectivity but lower

Table 2. Screening conditions for the $Al(C_6F_5)_3$ -catalysed ring opening.

Entry	Solvent	Conv. ^[a] (%)	3aa	4aa	5aa
1	DCM	100	84	0	16
2 ^[b]	DCM	100	79	0	21
3	DCE	75	79	0	21
4	$CHCl_3$	83	91	0	9
5	THF	78	88	0	12
6	TBME	79	90	0	10
7	Toluene	97	87	0	13
8 ^[c]	Toluene	100	46	0	53
9 ^[d]	Toluene	100	93	0	7
10 ^[d,e]	Toluene	100	93 (76)^[f]	0	7
11 ^[e,g]	Toluene	100	93	0	7

^[a] Determined by ¹H-NMR.

^[b] 0.2 M.

^[c] At 0 °C.

^[d] At 40 °C.

^[e] Using 1 mol%.

^[f] Isolated yield (%).

^[g] Stock solution.

conversions. In an attempt to avoid coordinating solvents and taking into account the LA employed, we used toluene which gave comparable selectivity and conversion to DCM (entry 7). Furthermore, the temperature played a role, with higher dimer formation for the reaction at 0 °C (entry 8) and lower at 40 °C (entry 9) due to entropic factors. As expected, higher concentrations (entry 2) favoured dimerization. Finally, the catalyst loading could be lowered to 1 mol% without compromising the selectivity. As a result, we enhanced the selectivity ratio of **3a/5a** (93% of the homoallylic alcohol **3a**) with a 76% isolated yield (entry 10). The difference between the NMR conversion and the isolated yield is explained mainly by the volatility of the product. To avoid the manipulation of the reported thermally sensitive compound, we used a stock solution in toluene (entry 11) which afforded the same regioselectivity.

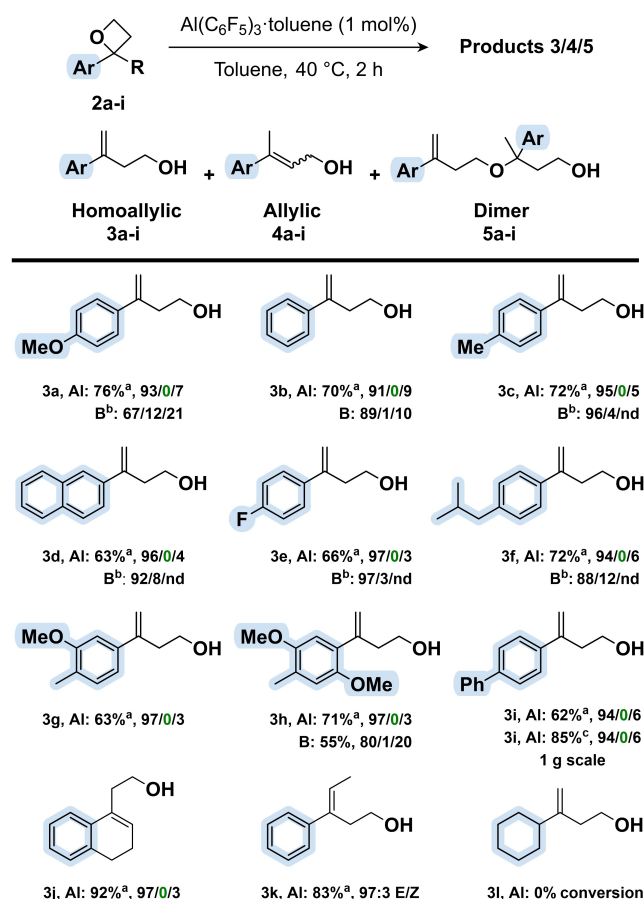
At this point, we sought to broaden the substrate scope in the regioselective ring-opening reaction. With the chromatography-purified oxetanes in hand, we explored the substrate scope modifying the aryl group with a range of functional groups, specially focusing on electron-donating (EDG) substituents (Scheme 3).

Oxetanes **2a** and **2c**, with EDG (*p*-OMe-Ph, *p*-Me-Ph), and **2b** (Ph) afforded total selectivity towards the homoallylic alcohols **3a–c** and less than 9% of dimer (yields ranging from 62 to 92%). Oxetanes bearing naphthyl (**2d**), *p*-F-Ph (**2e**) and *p*-iBu-Ph (**2f**) which purification from the allylic regioisomers was difficult, also afforded complete selectivity since the allylic alcohols **4d–f** were not detected by NMR. The reaction tolerated EWG (**3e** and **3i**), different alkyl substituents (**3j** and **3k**) as well as multiple electron-donating patterns such as in **3g** and **3h**. As expected, the non-aromatic substrate **21** showed no conversion towards alcohol **3l**. Additionally, we could perform a one gram scale synthesis of **3i** with 85% yield from the freshly prepared stock solution.

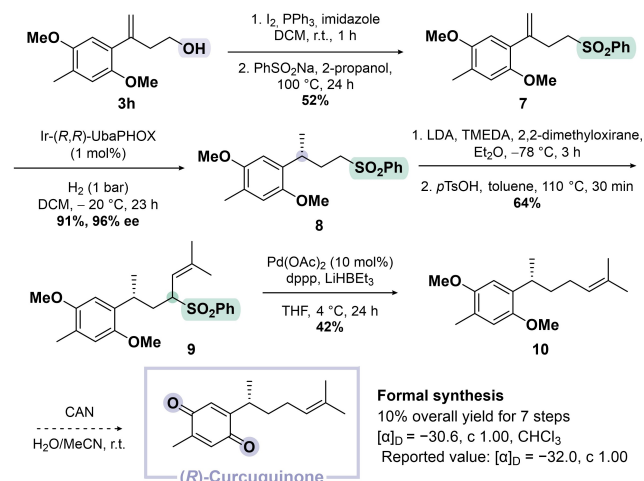
To showcase the applicability of the synthetic methodology, we undertook the syntheses of two distinct chiral products namely (*R*)-curcuquinone and (*R*)-RC-33. These compounds share the chiral α -methyl aromatic fragment, which is present in many marketed drugs. The synthetic routes focus on the introduction of chirality by Ir-catalyzed asymmetric hydrogenation, using the commercially available Ir-UbaPHOX ligand.^[38]

(*R*)-Curcuquinone belongs to the bisabolene family of sesquiterpenes which have attested antimicrobial and antifungal properties.^[39] Among this group of compounds, we have recently enantioselectively synthesized (*R*)-curcumene.^[30] Based on a similar strategy, we envisioned the formal synthesis of (*R*)-curcuquinone in 7 steps (Scheme 4).

Starting from homoallylic alcohol **3h**, transformation to the iodide through an Appel reaction and



Scheme 3. Substrate scope in the $\text{Al}(\text{C}_6\text{F}_5)_3$ -catalysed isomerization. Al= $\text{Al}(\text{C}_6\text{F}_5)_3$; B= $\text{B}(\text{C}_6\text{F}_5)_3$. ^{a)} Yield of the isolated products. ^{b)} Previously reported.^[29] ^{c)} gram scale.

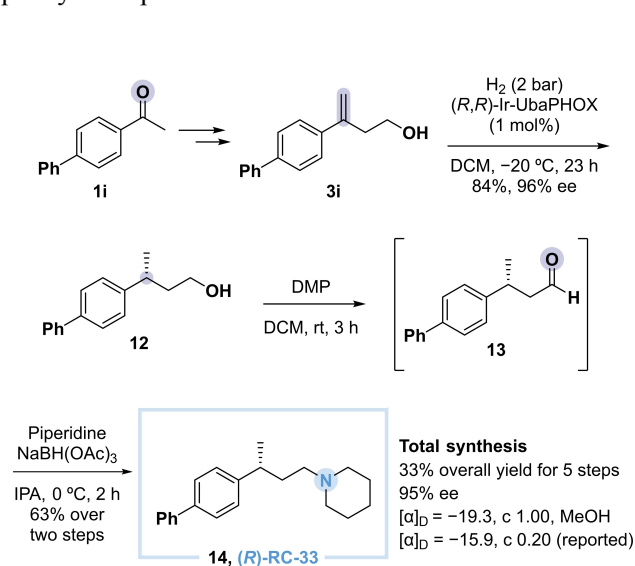


Scheme 4. Formal synthesis of (*R*)-curcuquinone.

subsequent treatment with sodium phenyl sulfinate afforded homoallylic sulfone **7** in two steps with 52% yield. Asymmetric hydrogenation of the sulfone with Ir-UbaPHOX afforded **8** in excellent yield and

enantioselectivity (91%, 96% ee). Then, LDA deprotonation, treatment with 2,2-dimethyloxirane and dehydration afforded a 2:1 mixture of diastereomeric sulfones **9** (64% yield, Scheme 4). We continued the synthesis with the mixture because the new stereocenter would be removed later. The last step was the desulfonylation, however, instead of using recurring sodium amalgam,^[40] we introduced a catalytic step based on the formation of a π -allylpalladium complex.^[41] This complex was attacked by superhydride to afford **10** in 42% yield. The oxidation of this intermediate to curcuquinone has previously been described.^[42] The absolute configuration was confirmed by optical rotation ($[-30.6, c=1.05, \text{CHCl}_3]$) which matched the reported value ($[-32.0, c=1.00, \text{CHCl}_3]$).^[43] Therefore, we achieved a formal synthesis of (*R*)-(-)-curcuquinone with a 10% total yield in 7 steps.

(*R*)-RC-33 has shown promising biological activity as agonists towards the activation of σ_1 receptors.^[44,45] These receptors have garnered attention as potential therapeutic targets for a range of neurological disorders, such as drug addiction, cancer, and neurodegenerative diseases.^[46] To date, RC-33 has already been synthesized by Ir-catalysed asymmetric hydrogenation, under high pressure.^[44] However, those authors reported an enantiomeric excess of 95%, after recrystallization. In this work, we envisioned the synthesis of the potent (*R*)-RC-33 σ_1 receptor agonist, using the homoallylic alcohol **3i** as a building block. Asymmetric hydrogenation of alcohol **3i** at -20°C and 2 barg of hydrogen afforded **12** in 84% yield and 96% ee (Scheme 5). Dess-Martin oxidation to the corresponding aldehyde **13**,^[47] followed by the reductive amination afforded the desired drug **14** in 33% overall yield in 5 steps starting from commercially available 4-phenylacetophenone **1i**.^[48]

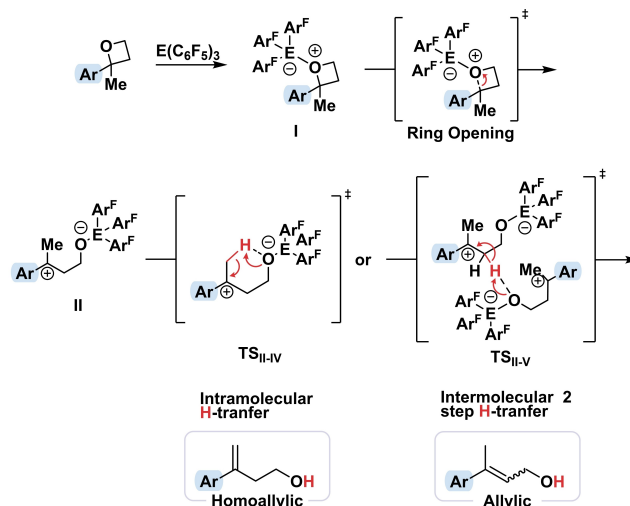


Scheme 5. Enantioselective total synthesis of RC-33.

The enantiomeric purity was found to be 95% ee as determined by chiral HPLC without the need for recrystallization. This was confirmed by the optical rotation ($[-19.3, c=1.00, \text{MeOH}; -30.6, c=1.00, \text{CHCl}_3]$) which was consistent with the literature ($[-15.9, c=0.20, \text{MeOH}]$).^[44] As a result, we have disclosed the total synthesis of (*R*)-RC-33 which, to our knowledge, is the shortest and most efficient route reported to date. Moreover, our approach allows the synthesis of either enantiomer with high stereochemical purity, starting from the achiral homoallylic alcohol **3i**.

In a previous study we analyzed, by means of DFT calculations, the mechanism of formation of the homoallylic and allylic products mediated by $\text{B}(\text{C}_6\text{F}_5)_3$ (Scheme 6, Ar=Ph; E=B).^[29] In the present work we have computed the mechanisms from oxetane **2a**, using $\text{B}(\text{C}_6\text{F}_5)_3$ and $\text{Al}(\text{C}_6\text{F}_5)_3$ (Scheme 6, Ar=*p*-MeOPh-, E=B or Al). Moreover, in addition to these two already known pathways, for both $\text{B}(\text{C}_6\text{F}_5)_3$ and $\text{Al}(\text{C}_6\text{F}_5)_3$ catalysts and **2a** substrate (Ar=*p*-MeOPh-), we have investigated the mechanism for the formation of the dimer by-product **5a**, to disclose the origin of the selectivity and rationalize the reduced formation of this by-product with aluminum catalyst.

Several routes, with a thorough exploration of the conformational space and location of intermediates and transition states, were investigated using the B3LYP-D3 functional with basis set BS1 and including dichloromethane solvent (DCM) in the optimizations through the SMD implicit solvent method. To obtain accurate energies, additional single-point calculations were performed on all optimized structures using the domain-based local pair natural orbital coupled cluster approach (DLPNO-CCSD(T)) and an



Scheme 6. Computed mechanism for the formation of homoallylic and allylic products (E=B, ref. [29]; E=Al, present work).

extended basis set (def2-TZVP) (see extended computational details in the Supporting Information).^[49] This method can be considered the state-of-the-art for providing energies of systems of this size, and it has proved to be very effective in obtaining accurate reaction thermodynamics and barrier heights. All of the Gibbs energies collected in the text have been obtained, adding to the DLPNO-CCSD(T)/def2-TZVP electronic energies thermal and entropic corrections as well as solvation energies ($\Delta G(\text{solv})$) obtained at the B3LYP-D3/BS1 optimization level.

Despite reactions with $\text{B}(\text{C}_6\text{F}_5)_3$ and $\text{Al}(\text{C}_6\text{F}_5)_3$ proceed with the same mechanism, the relative energies of the species involved are different. Complete Gibbs energy profiles can be found at the Supporting Information (Figures S1 and S2), as well as the optimized structures of all the intermediates and transition states. Here we will comment their main features, focusing on the competition between homoallylic and dimeric products.

The shape of the Gibbs energy profiles for boron and aluminum reagents is very similar, but with much lower relative energies for aluminum containing species. Our DFT studies showed that the formation of all the products (the homoallylic and the allylic alcohols and the dimer) first require ring opening of the oxetane **I**, promoted by interaction with the Lewis acid. The zwitterionic intermediates with the open ring **II** are formed in this step. The ring opening step of the electron rich **2a** oxetane does not affect the product ratio and for both boron and aluminum catalysts it has a very low barrier. However, the strongest Lewis acidity of $\text{Al}(\text{C}_6\text{F}_5)_3$ is reflected in the relative Gibbs energy of the zwitterionic intermediates: whereas **II-B** is stabilized $9.0 \text{ kcal mol}^{-1}$ with respect separated reagents, **II-Al** falls $26.4 \text{ kcal mol}^{-1}$ below the separated species. The same happens with all the species in the energy profiles.

Proton transfer of a C–H proton to the basic oxygen atom of the intermediate **II** generates the homoallylic and allylic products. As we showed in our previous study, **II** can evolve in two ways: (a) **intramolecular pathway**, in which a proton is transferred from methyl to oxygen directly generating the homoallylic product; (b) **intermolecular two step pathway**, in which first a C_βH_2 proton is transferred to the oxygen of another **II** intermediate, that in a second step give back the proton to the oxygen of the first unit generating the allylic alcohol (Scheme 6). For both $\text{Al}(\text{C}_6\text{F}_5)_3$ and $\text{B}(\text{C}_6\text{F}_5)_3$ catalysts formation of allylic alcohols implies higher barriers than formation of homoallylic product (see Figures S1 and S2). The selectivity towards the homoallylic alcohol is, therefore, well reproduced in both cases.

The lower dimerization observed with the aluminum catalysts was much harder to reproduce. The key barriers that can justify the experimental differences

between boron and aluminum LA catalysts are collected in Table 3.

The barrier for the formation of the homoallylic product is decided at transition state **TS_{III-IV}** involving intramolecular H-transfer. The formation of dimeric side-product also involves the very reactive intermediate **II** and it is a stepway process: it should entail the attack of the oxygen of the homoallylic product to the electrophilic carbon of **II** (**TS_{III-IV'}**)^[50] followed by a proton migration from the oxygen of the protonated ether to the terminal oxygen bonded to the Lewis acid (**TS_{IV'-V'}**).^[51]

After exploring several possibilities, we have found that the favoured pathway for the dimerization implies, in addition to the homoallylic product, the cooperation of two units of intermediate **II**. The C–O bond formation and the deprotonation of O-ether takes place concertedly, with the proton being transferred to the second **II** unit (Scheme 7, **TS_{III-IV'}**). Then the protonated **II** transfers back the proton to the terminal oxygen of the first unit (through **TS_{IV'-V'}**) leading to the formation of the dimer **5a** (Scheme 7). This second step has lower barrier than the first one and does not influence the product ratio.

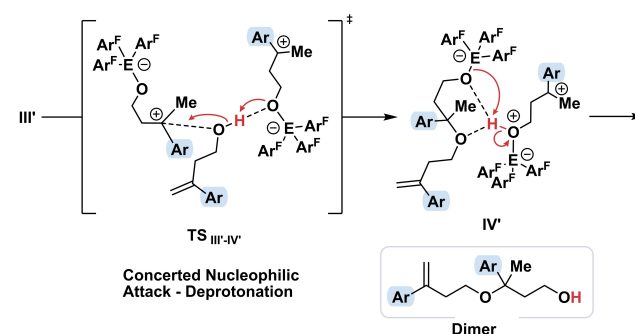
The competition between homoallyl alcohol and dimer formation is governed by the energy difference between transition states **TS_{III-IV}** (intramolecular proton

Table 3. Comparison of key barriers (in kcal mol^{-1}) for $\text{B}(\text{C}_6\text{F}_5)_3$ and $\text{Al}(\text{C}_6\text{F}_5)_3$ -catalysed formation of the homoallylic and dimer products.

	TSs	$\Delta G^\ddagger_{\text{DCM}} \text{ [a]}$	$\Delta\Delta G^\ddagger_{\text{DCM}} \text{ [a,b]}$
Homoallylic	TS_{III-IV-B}	16.0	2.6
Dimer (1st step)	TS_{III-IV'-B}	18.6	
Dimer (2nd step)	TS_{IV'-V'-B}	13.0	
Homoallylic	TS_{III-IV-Al}	17.7	3.0
Dimer (1st step)	TS_{III-IV'-Al}	20.7	
Dimer (2nd step)	TS_{IV'-V'-Al}	12.7	

[a] DLPNO-CCSD(T) computed Gibbs energy barriers.

[b] Gibbs energy difference between homoallylic and dimer competitive transition states (TSs) highlighted in bold.



Scheme 7. Computed mechanism for the formation of dimer.

transfer) and $\text{TS}_{\text{III}^{\cdot}\text{IV}^{\cdot}}$ (concerted nucleophilic attack-deprotonation). This difference amounts $2.6 \text{ kcal mol}^{-1}$ for $\text{Al}(\text{C}_6\text{F}_5)_3$ and $3.0 \text{ kcal mol}^{-1}$ for $\text{B}(\text{C}_6\text{F}_5)_3$.

Overall, these results justify the lower ratio of **5a** by-product obtained with $\text{Al}(\text{C}_6\text{F}_5)_3$ (**3a:5a** products: 88:8 (A) vs. 67:21 (B), Table 1). From these experimental values the difference should be around 1 kcal mol^{-1} . The computed value is not far from this value.

Conclusion

Here we developed an improved methodology for the oxetane ring-opening by using $\text{Al}(\text{C}_6\text{F}_5)_3$, as the Lewis superacid. A wide range of oxetanes (12 examples) were isomerized towards the homoallylic product, completely avoiding the formation of the allylic regioisomers, and reducing the formation of a dimer by-product (3–9%). The procedure is especially convenient for substrates with EDG such as methoxy, alkyl or aryl. The decrease of the dimer formation highly improved the preparation of the starting material for the enantioselective formal synthesis of (*R*)-(–)-curcuquinone (96% ee, seven steps from the homoallyl alcohol, 10% overall yield). Moreover, the total synthesis of the σ_1 receptor agonist, (*R*)-RC-33, was conducted in only five steps from 4-phenylacetophenone (95% ee, of 33% overall yield). DFT calculations provided a mechanistic insight into this transformation allowing us to understand the regioselectivity as well as the formation of the dimeric species.

Experimental Section

Preparation of $\text{Al}(\text{C}_6\text{F}_5)_3$ as a Toluene Adduct^[33]

In a glovebox, $\text{B}(\text{C}_6\text{F}_5)_3$ (0.51 g, 1 mmol, 1 equiv.) was weighted in a 25 mL Schlenk tube and dissolved in 1 mL of anhydrous toluene. The reaction mixture was left stirring for 1 min and then 2 mL of previously sparged hexane were added. After 20 min stirring at rt, 0.5 mL of AlMe_3 (2.0 M in toluene, 1 mmol, 1 equiv.) was added to the resulting suspension dropwise. The solution became transparent once all AlMe_3 was added and after 20 min a white precipitate appeared. The suspension was left stirring overnight at room temperature. The Schlenk tube was evacuated and purged with nitrogen (x3) to remove BMe_3 (gas) and the supernatant was removed with a syringe under a positive pressure of N_2 . The remaining solid was washed with cold hexane (x2) and finally dried under reduced vacuum to afford $\text{Al}(\text{C}_6\text{F}_5)_3 \cdot \text{tol}$ as a white solid in 68% yield. The compound was stored in the freezer of the glovebox.

^{19}F -NMR (376 MHz, C_6D_6) δ –123.8 (d, $J=18.7 \text{ Hz}$, 6F), –151.4 (t, $J=18.8 \text{ Hz}$, 3F), –161.1 (m, 6F) ppm. The analytical data for this compound was in excellent agreement with the reported data.^[33]

General Procedure for the Preparation of Homoallylic Alcohols

A sealed capped vial with a stirring bar was taken into the glovebox and $\text{Al}(\text{C}_6\text{F}_5)_3 \cdot \text{tol}$ (3 mg, 0.006 mmol, 0.01 equiv.) was weighted and dissolved in anhydrous toluene (0.5 mL). It was then added to a solution of the corresponding oxetane **2a–i** (0.4 mmol, 1.0 equiv.) in toluene (3.5 mL, 0.1 M) at 40°C while stirring for 2 hours. Afterwards, water was added, and the two resulting layers were separated. The aqueous layer was extracted with DCM (x3), the combined organic layers were dried over MgSO_4 , and the solvent was evaporated under reduced pressure. Ratios between compounds **3**, **4** and **5a–i** were determined by ^1H NMR of the crude mixture. The product was further purified by flash column chromatography.

Safety

Caution! $\text{Al}(\text{C}_6\text{F}_5)_3 \cdot \text{toluene}$ is potentially shock and thermally sensitive due to the formation of benzyne intermediate upon heating. Handle this material under strict inert atmosphere and do not heat it in a close compartment without solvent. We recommend to use a stock solution in toluene

Acknowledgements

This work was supported by grants from FEDER/Ministerio de Ciencia e Innovación (MICINN) PID2020-115074GB-I00/AEI/10.13039/501100011033 to A.R. and X.V. and PID2020-116861GB-I00 (to A.L.). IRB Barcelona is the recipient of institutional funding from MICINN through the Centres of Excellence Severo Ochoa Award and from the CERCA Program of the Catalan Government. We thank the Generalitat de Catalunya for grant 2021 SGR 00866 and for a predoctoral fellowship (M.B.). Calculations were carried out using CSUC high-performance computing resources.

References

- [1] C. Masters, *Homogeneous Transition-metal Catalysis*, Springer Netherlands, Dordrecht, 1980.
- [2] S. Bhaduri, D. Mukesh, *Homogeneous Catalysis*, Wiley: Hoboken, NJ, 2014.
- [3] J. Pospech, I. Fleischer, R. Franke, S. Buchholz, M. Beller, *Angew. Chem. Int. Ed.* **2013**, 52, 2852–2872.
- [4] O. Sereda, S. Tabassum, R. Wilhelm, Lewis Acid Organocatalysts. In *Asymmetric Organocatalysis. Topics in Current Chemistry*; B. List, Ed.; Springer: Berlin, Heidelberg, 2010; Vol. 291, pp. 86–117.
- [5] G. N. Lewis, *J. Am. Chem. Soc.* **1916**, 38, 762–785.
- [6] G. A. Olah, G. K. S. Prakash, J. Sommer, *Science* **1979**, 206, 13–20.
- [7] L. O. Müller, D. Himmel, J. Stauffer, G. Steinfeld, J. Slattery, G. Santiso-Quinones, V. Brecht, I. Krossing, *Angew. Chem. Int. Ed.* **2008**, 47, 7659–7663.
- [8] L. Greb, *Chem. Eur. J.* **2018**, 24, 17881–17896.


- [9] S. Aldridge, A. J. Downs, *The Group 13 Metals Aluminum, Gallium, Indium and Thallium: Chemical Patterns and Peculiarities*, Wiley, 2011.
- [10] L. A. Mück, A. Y. Timoshkin, G. Frenking, *Inorg. Chem.* **2012**, *51*, 640–646.
- [11] I. V. Kazakov, A. S. Lisovenko, N. A. Shcherbina, I. V. Korniyakov, N. Y. Gugin, Y. V. Kondrat'ev, A. M. Chernysheva, A. S. Zavgorodnii, A. Y. Timoshkin, *Eur. J. Inorg. Chem.* **2020**, *47*, 4442–4449.
- [12] T. Kähler, R. L. Melen, *Cell Rep. Phys. Sci.* **2021**, *2*, 100595.
- [13] T. Belgardt, J. Storre, H. W. Roesky, M. Noltemeyer, H.-G. Schmidt, *Inorg. Chem.* **1995**, *34*, 3821–3822.
- [14] J. L. W. Pohlmann, F. E. Brinckmann, *Z. Naturforsch. B* **1965**, *20*, 5–11.
- [15] G. S. Hair, A. H. Cowley, R. A. Jones, B. G. McBurnett, A. Voigt, *J. Am. Chem. Soc.* **1999**, *121*, 4922–4923.
- [16] See for instance: a) L. Cai, B. Liu, X. Liu, D. Cui, *Polymer* **2022**, *241*, 124539; b) J. W. Baek, J. H. Ko, J. H. Park, J. Y. Park, H. J. Lee, Y. H. Seo, J. Lee, B. Y. Lee, *Organometallics* **2022**, *41*, 2455–2465; c) E. A. Ison, J. L. Tubb, *Inorg. Chem.* **2021**, *60*, 13797–13805; d) Y. Wan, W. Zhao, H. Zhao, M. Zhou, J. He, Y. Zhang, *Macromolecules* **2023**, *56*, 7763–7770; e) L. Cai, Q. Y. Wang, X. L. Liu, D. M. Cui, *Chin. J. Polym. Sci.* **2023**, *41*, 713–719; f) M. J. Krahfuss, U. Radius, *Eur. J. Inorg. Chem.* **2021**, 548–561.
- [17] a) A. Y. Timoshkin, G. Frenking, *Organometallics* **2008**, *27*, 371–380; b) H. Böhrer, N. Trapp, D. Himmel, M. Schleep, I. Krossing, *Dalton Trans.* **2015**, *44*, 7489–7499; c) L. A. Mück, A. Y. Timoshkin, G. Frenking, *Inorg. Chem.* **2012**, *51*, 640–646; d) E. I. Davydova, T. N. Sevastianova, A. Y. Timoshkin, *Coord. Chem. Rev.* **2015**, *297*, 91–126.
- [18] A. Y. Timoshkin, *Chem. Eur. J.* **2024**, *30*, e202302457.
- [19] A. Chardon, A. Osi, D. Mahaut, T. H. Doan, N. Tumanov, J. Wouters, L. Fusaro, B. Champagne, G. Berionni, *Angew. Chem. Int. Ed.* **2020**, *59*, 12402–12406.
- [20] J. D. Gorden, A. Voigt, C. L. B. Macdonald, J. S. Silverman, A. H. Cowley, *J. Am. Chem. Soc.* **2000**, *122*, 950–951.
- [21] A. Cabré, G. Sciortino, G. Ujaque, X. Verdager, A. Lledós, A. Riera, *Org. Lett.* **2018**, *20*, 5747–5751.
- [22] A. Cabré, J. Cabezas-Giménez, G. Sciortino, G. Ujaque, X. Verdager, A. Lledós, A. Riera, *Adv. Synth. Catal.* **2019**, *361*, 3624–3631.
- [23] M. R. Bauer, P. Di Fruscia, S. C. C. Lucas, I. N. Michaelides, J. E. Nelson, R. I. Storer, B. C. Whitehurst, *RSC Med. Chem.* **2021**, *12*, 448–471.
- [24] S. Ahmad, M. Yousaf, A. Mansha, N. Rasool, A. F. Zahoor, F. Hafeez, S. M. A. Rizvi, *Synth. Commun.* **2016**, *46*, 1397–1416.
- [25] See for instance: a) C. J. Whiteoak, E. Martin, M. M. Belmonte, J. Benet-Buchholz, A. W. Kleij, *Adv. Synth. Catal.* **2012**, *354*, 469–476; b) J. Rintjema, W. Guo, E. Martin, E. C. Escudero-Adán, A. W. Kleij, *Chem. Eur. J.* **2015**, *21*, 10754–10762; c) W. Guo, V. Laserna, J. Rintjema, A. W. Kleij, *Adv. Synth. Catal.* **2016**, *358*, 1602–1607.
- [26] a) A. Gansäuer, N. Ndene, T. Lauterbach, J. Justicia, I. Winkler, C. Mück-Lichtenfeld, S. Grimme, *Tetrahedron* **2008**, *64*, 11839–11845; b) N. Takekoshi, K. Miyashita, N. Shoji, S. Okamoto, *Adv. Synth. Catal.* **2013**, *355*, 2151–2157.
- [27] a) Y. Tang, C. Shen, Q. Yao, X. Tian, B. Wang, K. Dong, *ChemCatChem* **2020**, *12*, 5898–5902; b) F. G. Delolo, J. Fessler, H. Neumann, K. Junge, E. N. dos Santos, E. V. Gusevskaya, M. Beller, *J. Mol. Catal.* **2022**, *530*, 112621.
- [28] J. A. Bull, R. A. Croft, O. A. Davis, R. Doran, K. F. Morgan, *Chem. Rev.* **2016**, *116*, 12150–12233.
- [29] A. Cabré, S. Rafael, G. Sciortino, G. Ujaque, X. Verdager, A. Lledós, A. Riera, *Angew. Chem. Int. Ed.* **2020**, *132*, 7591–7597.
- [30] M. Bellido, C. Riego-Mejias, A. Diaz-Moreno, X. Verdager, A. Riera, *Org. Lett.* **2023**, *25*, 1453–1457.
- [31] K. Okuma, Y. Tanaka, S. Kaji, H. Ohta, *J. Org. Chem.* **1983**, *48*, 5133–5134.
- [32] J. Chen, E. Y. X. Chen, *Dalton Trans.* **2016**, *45*, 6105–6110.
- [33] S. Feng, G. R. Roof, E. Y. X. Chen, *Organometallics* **2002**, *21*, 832–839.
- [34] N. G. Stahl, M. R. Salata, T. J. Marks, *J. Am. Chem. Soc.* **2005**, *127*, 10898–10909.
- [35] Z. Liu, X.-S. Tu, L.-T. Guo, X.-C. Wang, *Chem. Sci.* **2020**, *11*, 11548–11553.
- [36] D. Chakraborty, E. Y.-X. Chen, *Inorg. Chem. Commun.* **2002**, *5*, 698–701.
- [37] A. Jordan, C. G. J. Hall, L. R. Thorp, H. F. Sneddon, *Chem. Rev.* **2022**, *122*, 6749–6794.
- [38] F. Menges, A. Pfaltz, *Adv. Synth. Catal.* **2002**, *344*, 40–44.
- [39] C. Fuganti, S. Serra, *J. Chem. Soc. Perkin Trans. 1* **2000**, 3758–3764.
- [40] C. K. Chan, Y. H. Huang, M. Y. Chang, *Tetrahedron* **2016**, *72*, 5521–5529.
- [41] R. O. Hutching, K. Learn, *J. Org. Chem.* **1982**, *47*, 1380–1382.
- [42] T. Yoshimura, H. Kisyuku, T. Kamei, K. Takabatake, M. Shindo, K. Shishido, *Arkivoc* **2003**, *8*, 247–255.
- [43] V. K. Aggarwal, L. T. Ball, S. Carobene, R. L. Connelly, M. J. Hesse, B. M. Partridge, P. Roth, S. P. Thomas, M. P. Webster, *Chem. Commun.* **2012**, *48*, 9230–9232.
- [44] D. Rossi, A. Pedrali, A. Marra, L. Pignataro, D. Schepmann, B. Wünsch, L. Ye, K. Leuner, M. Peviani, D. Curti, O. Azzolina, S. Collina, *Chirality* **2013**, *25*, 814–822.
- [45] D. Rossi, A. Pedrali, R. Gaggeri, A. Marra, L. Pignataro, E. Laurini, V. DalCol, M. Fermeiglia, S. Priol, D. Schepmann, B. Wünsch, M. Peviani, D. Curti, S. Collina, *ChemMedChem* **2013**, *8*, 1514–1527.
- [46] T. Maurice, T. P. Su, *Pharmacol. Ther.* **2009**, *124*, 195–206.
- [47] D. B. Dess, J. C. Martin, *J. Org. Chem.* **1983**, *48*, 4155–4156.

- [48] A. F. Abdel-Magid, K. G. Carson, B. D. Harris, C. A. Maryanoff, R. D. Shah, *J. Org. Chem.* **1996**, *61*, 3849–3862.
- [49] For extended computational details, see Supporting Information.
- [50] Transition states $\text{TS}_{\text{III-IV}}$ correspond to transition states for the **II** to **IV** intramolecular proton transfer in which an additional molecule of **II** has been included to allow energy comparison with the intermolecular proton transfer. See optimized structures in the Supporting Information.
- [51] Transition states and minima marked as prime (**III'**, $\text{TS}_{\text{III'-IV'}}$, **IV'** and **V'**) indicate participation of a second molecule of homoallyl alcohol **3a**.

RESEARCH ARTICLE

Regioselective Ring-Opening of Oxetanes Catalyzed by Lewis Superacid $\text{Al}(\text{C}_6\text{F}_5)_3$

Adv. Synth. Catal. **2024**, 366, 1–10

 M. Bellido, C. Riego-Mejías, G. Sciortino, X. Verdager*, A. Lledós*, A. Riera*

